Journal of Membrane Science Letters 5 (2025) 100110

Contents lists available at ScienceDirect

Journal of Membrane Science Letters

journal homepage: www.elsevier.com/locate/memlet

Fabrication and property modification of free-standing PSS/PDADMAC ultra- and microfiltration membranes by incorporating cellulosic additives

Ang Zhao [a], Lea Erbacher [a], Prasath Paskaran [a], Matthias Wessling [a,b,*]

[a] Chemical Process Engineering AVT.CVT, RWTH Aachen University, Forckenbeckstraße 51, 52074 Aachen, Germany
[b] DWI - Leibniz-Institute for Interactive Materials, Forckenbeckstraße 50, 52074 Aachen, Germany

ARTICLE INFO

Keywords:
Ultra-/microfiltration membranes
Polyelectrolyte complexes
Sustainable aqueous phase separation
STMP crosslinking
Cellulosic additive

ABSTRACT

In classical membrane fabrication, water-soluble additives such as polyvinylpyrrolidone (PVP) have been pivotal in generating porosity and tuning surface properties. By contrast, comparable modifiers for membranes produced via all-aqueous processes – such as polyelectrolyte complex (PEC) membranes – remain largely unexplored. Here, we demonstrate that hydroxyethyl cellulose (HEC) and hydroxypropyl cellulose (HPC) act as effective pore formers and structural modifiers in PEC flat-sheet membranes prepared by salt-dilution-induced phase inversion. During fabrication, a fraction of the cellulosic additive is leached from the polymer solution, enhancing membrane porosity and permeability, while the residual fraction reinforces mechanical stability. Crosslinking with sodium trimetaphosphate (STMP) further strengthens the membranes. Membranes using HEC as the cellulosic additive exhibit a tunable increase in pure water permeability (from 43 ± 10 to 123 ± 47 LMH·bar^{-1}) and molecular weight cut-off (from 117 ± 64 to 460 ± 360 kDa). In addition, additive pretreatment and crosslinking strategies enable surface charge modulation, shifting it from positive to neutral or negative, and tailoring salt retention profiles. These findings establish cellulosic additives as versatile design elements in the emerging class of aqueous PEC membrane systems.

1. Introduction

Polyelectrolyte complex (PEC) membranes are increasingly recognized as a sustainable alternative to conventional membranes, owing to their fabrication in entirely aqueous media without the need for reprotoxic organic solvents (Durmaz et al., 2020; Kamp et al., 2021; Baig et al., 2020; Li et al., 2025). This solvent-free advantage positions PECs as promising candidates for next-generation separation technologies.

PECs form through the electrostatic complexation of oppositely charged polyelectrolytes (PEs), such as the strong polyanion poly(sodium-4-styrene sulfonate) (PSS) and the strong polycation poly(diallyldimethylammonium chloride) (PDADMAC) (Michaels, 1965; Shamoun et al., 2012; Wang and Schlenoff, 2014; Bediako et al., 2023). These combinations of materials can yield nanofiltration (NF) membranes via salt-dilution-induced phase separation (SIPS) (Emonds et al., 2021; Kamp et al., 2021). While this method enables entirely aqueous processing, the resulting membranes often suffer from limited mechanical robustness, which hinders their applicability in pressure-driven processes.

In classical membrane systems, water-soluble additives such as polyvinylpyrrolidone (PVP) have long been instrumental in tuning porosity and surface characteristics (Cabasso et al., 1976; Boom et al., 1992; Hwang and Sefton, 1995; Kim et al., 2001; Yoo et al., 2004). For aqueous PEC-based systems, however, comparable modifiers remain largely unexplored. In this study, we hypothesize that cellulosic polymers such as hydroxyethyl cellulose (HEC) and hydroxypropyl cellulose (HPC) can function as versatile additives in the fabrication of PSS/PDADMAC PEC membranes. Specifically, we propose that these additives serve a dual role: (i) acting as pore formers that are partially leached during salt-dilution-induced phase inversion, thereby enhancing porosity and permeability, and (ii) remaining partly embedded within the membrane matrix to reinforce mechanical integrity. Furthermore, we anticipate that pretreatment of the additives with sodium hydroxide (NaOH) will introduce negatively charged moieties, enabling controlled tuning of the membrane's surface charge. Finally, chemical crosslinking with sodium trimetaphosphate (STMP) is expected to synergistically improve robustness while modulating charge behavior. Together, these strategies provide a pathway to fabricate free-standing PEC membranes spanning the NF, ultrafiltration (UF), and microfiltration (MF) regimes with tunable structure, charge, and stability (see Fig. 1).

* Correspondence to: Forckenbeckstraße 51, 52074 Aachen, Germany.
E-mail address: Manuscripts.cvt@avt.rwth-aachen.de (M. Wessling).

https://doi.org/10.1016/j.memlet.2025.100110
Received 14 October 2025; Received in revised form 3 November 2025; Accepted 4 November 2025
Available online 6 November 2025

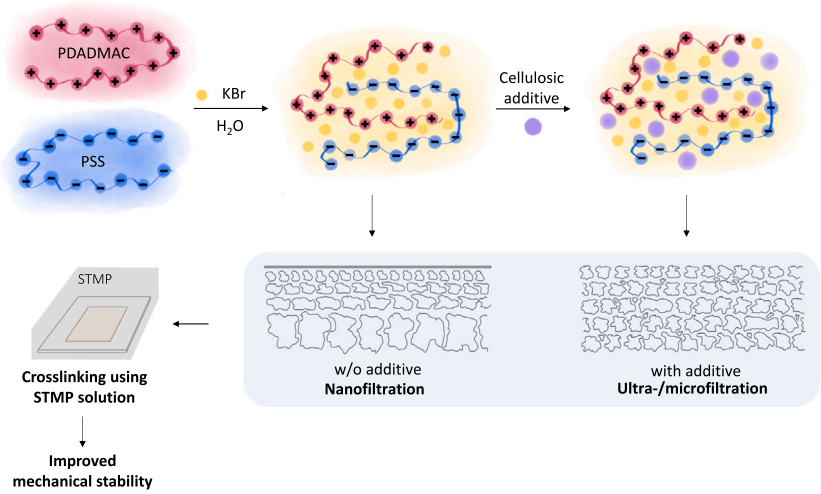

Fig. 1. Proposed fabrication process of flat-sheet PEC ultrafiltration membrane utilizing cellulosic additives to tailor porosity, mechanical strength and surface charge.

2. Experimental methods

PSS/PDADMAC membranes were fabricated as FS membranes using SIPS. HEC was added to the polymer solution at concentrations of 1 wt% or 2 wt% to produce UF or MF membranes, respectively. To improve the homogeneity of additive distribution and modify the membrane's surface charge, 1 wt% of NaOH-pretreated HEC or HPC (referred to as HEC-NaOH or HPC-NaOH) was incorporated into the polymer solution.

After precipitation of the PEC film in the aqueous coagulation bath, the membranes were crosslinked using STMP. Membranes labeled "-STMP" underwent subsequent post-treatment crosslinking in a separate STMP solution, whereas those labeled "-iCC" were subjected simultaneously to coagulation and crosslinking in a STMP coagulation bath. We subsequently characterized and compared the non-crosslinked membranes, the post-treated STMP-crosslinked membranes, and the coagulated STMP-crosslinked membranes. Detailed methods for membrane fabrication, crosslinking, and characterization processes can be found in the Supplementary Information (SI).

3. Results and discussion

3.1. Membrane morphology

The morphology of the fabricated PEC membranes was analyzed using cross-sectional field-emission scanning electron microscopy (FE-SEM), as shown in Fig. 2, to assess the effects of cellulosic additives and STMP crosslinking on membrane structure. Higher-resolution overview FESEM scans of the membrane's top layer are provided in the SI.

The reference membrane without additives (FS-Ref; Fig. 2a.1) displays an asymmetric architecture, consisting of a porous support matrix beneath a dense top layer. The support matrix features a uniform pore distribution, with pore sizes gradually decreasing toward the top, resulting in a smooth structural transition from the porous base to the dense skin layer.

Incorporating HEC as an additive into the polymer solution eliminated the dense top layer of the PEC membrane and significantly increased its overall porosity. The uncrosslinked membrane FS-1HEC (Fig. 2b.1) exhibits noticeably larger pores compared to FS-Ref. Furthermore, increasing the concentration of the cellulosic additive further enhanced membrane porosity. This also broadened the pore size distribution, as evident in FS-2HEC (Fig. 2c.1).

Using NaOH-pretreated HEC as an additive resulted in a reduction in pore size. The membrane FS-1HEC-NaOH (Fig. 2d.1) exhibits smaller pores than FS-1HEC. This decrease is attributed to the enhanced aqueous solubility of HEC following NaOH pretreatment, which enabled a more uniform distribution of the additive in the polymer solution. During phase inversion, this homogeneity facilitated a smoother washing-out process, ultimately yielding a membrane with finer pore structure.

In contrast, the incorporation of NaOH-pretreated HPC produced a porous membrane structure with numerous macrovoids that were unevenly distributed (FS-1HPC-NaOH; Fig. 2e.1). Unlike the HEC-based membranes, this membrane retained a dense top layer, which may act as a barrier to flow or introduce potential leakage points.

STMP crosslinking influenced membrane morphology, particularly in membranes containing NaOH-pretreated HPC. Post-treatment with STMP led to an increase in pore size. Compared to FS-1HPC-NaOH, the membrane FS-1HPC-NaOH-STMP exhibited a more porous structure with prominent open macrovoids (Fig. 2e.2). In contrast, direct coagulation in a 0.5 M STMP solution produced a markedly different morphology: FS-1HPC-NaOH-iCC (Fig. 2e.3) showed a significant reduction in overall thickness and a much denser, more compact structure.

Since membrane morphology and composition are closely linked to mechanical stability, we conducted tensile tests to evaluate the mechanical performance of the various membranes, as detailed in the Supplementary Information. Among all tested membranes, FS-Ref-STMP and FS-1HPC-NaOH-iCC exhibited the highest breaking stress, indicating that the incorporation of cellulosic additives, combined with STMP crosslinking, not only altered membrane structure but also significantly enhanced mechanical robustness. However, using HPC as a cellulosic additive tended to induce unevenly distributed macrovoids in the membrane structure, which should be considered in process optimization. Therefore, the procedure for incorporating HPC into the PEC system still needs improvement. Increasing the molecular weight of HPC might help reduce macrovoid formation.

3.2. Pure water permeability and molecular weight cut-off

NF membranes are typically characterized by a molecular weight cut-off (MWCO) ranging from 0.2 to 20 kDa and are capable of separating low-molecular-weight solutes such as salts, glucose, lactose, and micropollutants. UF membranes fall within an MWCO range of 20 to 200 kDa, while MF membranes exhibit MWCOs above 200 kDa and are suitable for separating particles larger than 0.1 μm (Koyuncu et al., 2015). To evaluate the filtration performance of the fabricated PEC membranes, their pure water permeability (PWP) and MWCO were measured.

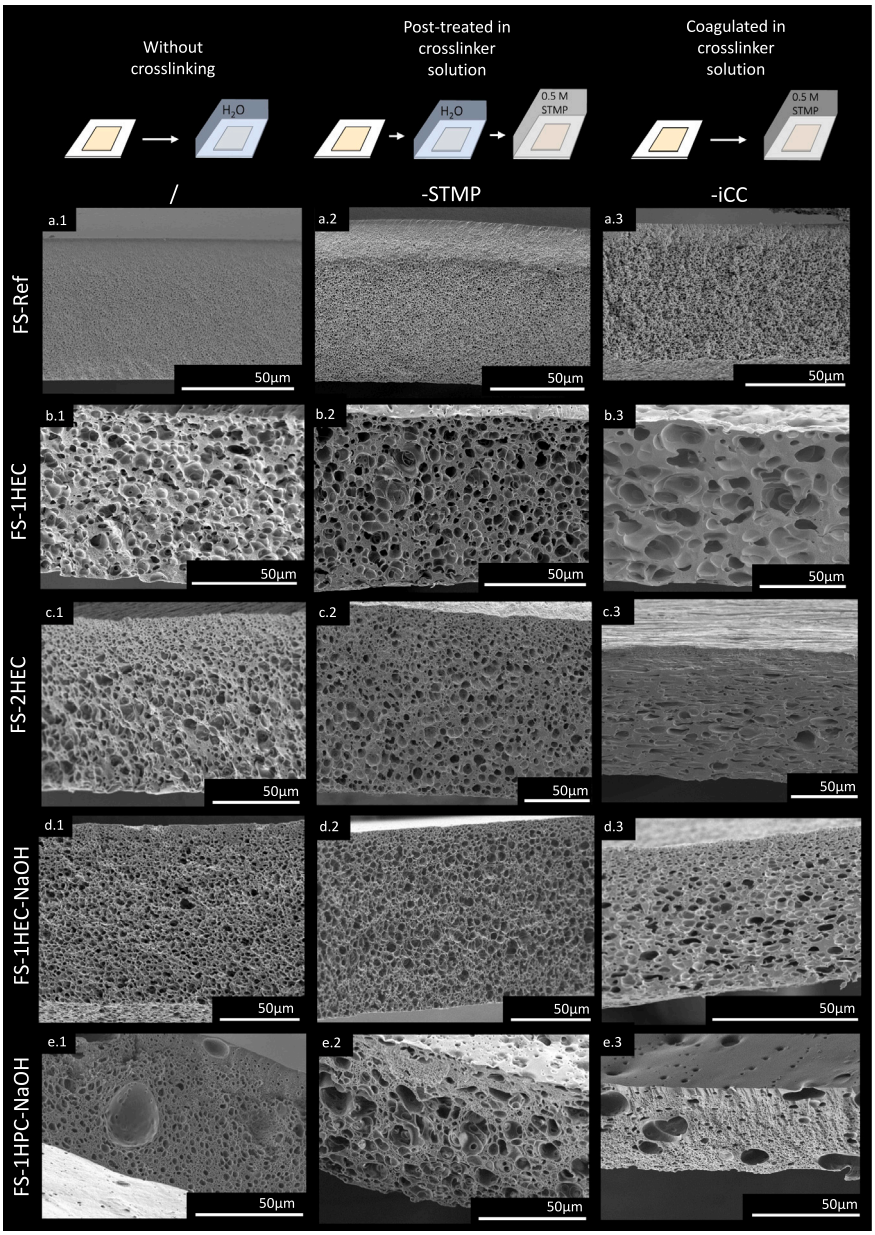

Fig. 2. Cross-sectional FESEM images of PEC membranes. (FS-Ref (a.1 - 3; membrane consists of PSS and PDADMAC without cellulosic additive); FS-1HEC (b.1 - 3; membrane consists of PSS and PDADMAC incorporated 1 wt% HEC); FS-2HEC (c.1 - 3; membrane consists of PSS and PDADMAC incorporated 2 wt% HEC); FS-1HEC-NaOH (d.1 - 3; membrane consists of PSS and PDADMAC incorporated 1 wt% NaOH-pretreated HEC); FS-1HPC-NaOH (e.1 - 3; membrane consists of PSS and PDADMAC incorporated 1 wt% NaOH-pretreated HPC)).

As shown in Fig. 3, both PWP and MWCO values increased with higher concentrations of additive in the polymer solution for membranes FS-Ref, FS-1HEC, FS-1HEC-NaOH, and FS-2HEC, indicating a linear trend.

The reference membrane FS-Ref exhibited a low PWP of 0.99 ± 0.08 LMH $\cdot$ bar^{-1} and an MWCO of 1.72 ± 0.02 kDa, placing it in the NF category. In contrast, FS-1HEC showed a markedly higher PWP of 43 ± 10 LMH $\cdot$ bar^{-1} and an MWCO of 117 ± 64 kDa, qualifying it as a UF membrane. FS-2HEC demonstrated the highest permeability, with a PWP of 123 ± 47 LMH $\cdot$ bar^{-1} and an MWCO of 460 ± 360 kDa, consistent with MF classification. The relatively large standard deviations in the PWP and MWCO values for FS-2HEC are likely due to the incomplete dispersion of HEC in the polymer solution, as it was not pretreated with NaOH to ensure full dissolution.

For comparison, FS-1HEC-NaOH – prepared with 1 wt% NaOH-pretreated HEC – achieved a PWP of 76 ± 16 LMH $\cdot$ bar^{-1} and an MWCO of 110 ± 10 kDa, values similar to FS-1HEC. However, the significantly reduced MWCO variability indicates that NaOH pretreatment of the additive improved solubility and distribution within the polymer solution, resulting in a more uniform pore structure. These findings are consistent with the morphological observations from FESEM analysis.

Among all fabricated membranes, FS-Ref, FS-Ref-STMP, FS-Ref-iCC, and FS-1HPC-NaOH-iCC exhibited NF properties, whereas the other membranes demonstrated measurable retention but no clear MWCO due to their broader or less selective pore distributions.

The complete list of all measured PWP and MWCO values are provided in SI Table 4. Rheological observations correlate with the PWP and MWCO trends of the fabricated membranes and mirror the function

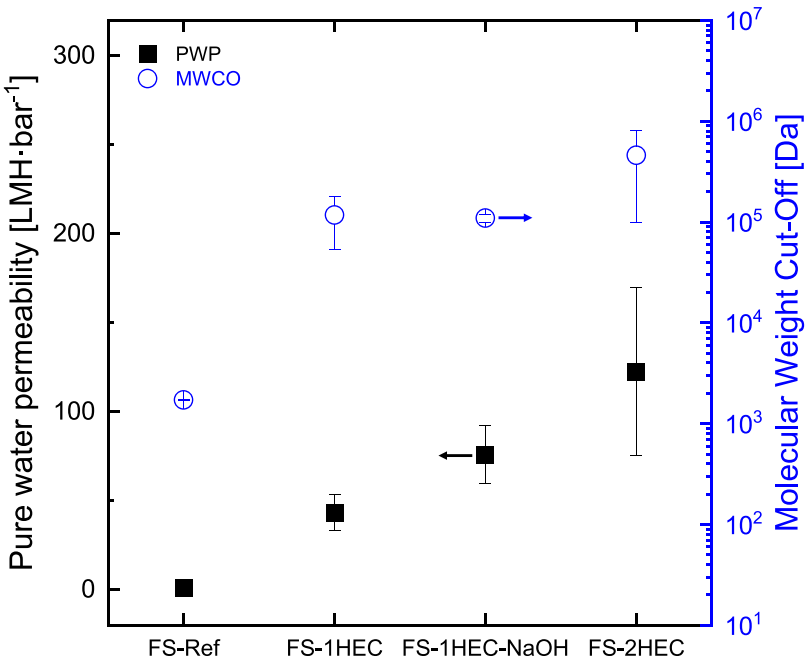

Fig. 3. PWP and MWCO of FS-Ref, FS-1HEC, FS-1HEC-NaOH, and FS-2HEC. The MWCO measurement was conducted at transmembrane pressure (TMP) of 1 bar.

of PVP in classical NIPS systems, indicating that the cellulosic additive facilitates pore formation and increases membrane porosity.

3.3. Zeta potential and salt retention

The zeta potential of the fabricated membranes was measured to assess the impact of cellulosic additives on membrane surface charge, as shown in Fig. 4 (1a.). The FS-Ref membrane (no additives) exhibited a positive surface charge across all measured pH values. Adding HEC (FS-1HEC) reduced the surface charge to nearly 0 mV between pH 4 and 9, indicating near-neutral behavior in this range. In contrast, pretreating the cellulosic additives HEC and HPC with 2 M NaOH introduced negatively charged –ONa groups, shifting the surface charge negative: FS-1HEC-NaOH was negative at all measured pH, while FS-1HPC-NaOH was negative at all pH except pH 3.

Crosslinking further modulated the surface charge (Fig. 4 (1b)). STMP crosslinking increased the charge magnitude compared with the non-crosslinked controls: FS-Ref-STMP was more positive across pH 4–9 than FS-Ref, whereas FS-1HPC-NaOH-STMP was more negative across pH 6–9 than FS-1HPC-NaOH. These effects likely arise from differences in the crosslinking route and the resulting membrane porosity. The PDADMAC/PSS ratio in the polymer solution was set to 1:1; ideally, one cationic group (PDADMAC) pairs with one anionic group (PSS), yielding a nominally charge-neutral matrix. However, the reference membrane (FS-Ref) without crosslinking exhibited a positive surface charge at this ratio, attributed to PDADMAC enrichment at the PEC top surface during coagulation, due to its lower molecular weight and hence higher mobility-relative to PSS (Kamp et al., 2021). STMP post-treatment further enhanced the positive surface charge because STMP interacts with and partially sequesters anionic sites on PSS, reducing the available negative charge to neutralize PDADMAC. Consequently, FS-Ref-STMP shows a more positive surface charge. In contrast, the uncrosslinked FS-1HPC-NaOH was negatively charged, and STMP crosslinking rendered the membrane highly porous. The resulting increase in negative surface charge for FS-1HPC-NaOH-STMP cannot therefore be attributed solely to crosslinking; membrane porosity also contributes. A more open, porous architecture tends to yield a stronger negative surface potential than a dense, compact layer (Yakin et al., 2020).

By contrast, coagulation crosslinking (iCC) attenuated the charge magnitude: FS-Ref-iCC was less positive and FS-1HPC-NaOH-iCC less negative than their respective non-crosslinked counterparts at all measured pH values except pH 3. We suspect that these phenomena may be explained by the crosslinking route and the resulting membrane porosity as well. In the coagulated STMP crosslinking procedure, the coagulation bath consisted of a 0.5 M STMP solution rather than DI water, thereby coupling crosslinking and coagulation. This route constrains PDADMAC chain rearrangement; as a result, PDADMAC remains more homogeneously distributed within the partially crosslinked PSS matrix, yielding a less positive surface charge. FS-1HPC-NaOH-iCC exhibits a less negative surface charge because coagulation crosslinking produces a denser, more compact membrane structure and, by crosslinking PSS and HPC-NaOH via STMP, consumes anionic sites, reducing the available negative charge relative to the uncrosslinked FS-1HPC-NaOH. Nevertheless, FS-Ref-STMP and FS-Ref-iCC remained positively charged across the measured pH range, while FS-1HPC-NaOH-STMP and FS-1HPC-NaOH-iCC remained negatively charged except at pH 3.

These molecular interpretations cannot be easily proven, they remain merely reasonable interpretations. Yet, the zeta potential results show that cellulosic additives tune membrane surface properties, shifting the charge from positive toward neutral or negative – especially when combined with NaOH pretreatment – whereas post-treated STMP crosslinking increases the charge magnitude (more positive or more negative) and coagulation crosslinking tends to shift the surface charge toward neutrality.

Salt retentions of the NF membranes FS-Ref, FS-Ref-STMP, FS-Ref-iCC, and FS-1HPC-NaOH-iCC were measured for $MgCl_2$, NaCl, $MgSO_4$, and Na_2SO_4 (Fig. 4 (2a.–2d.)). Using these four salts enables assessment of selectivity as a function of ion valence. FS-Ref, FS-Ref-STMP, and FS-Ref-iCC showed the highest retention for $MgCl_2$, whereas FS-1HPC-NaOH-iCC exhibited the highest retention for Na_2SO_4.

As shown in Fig. 4 (1b.), FS-Ref, FS-Ref-STMP, and FS-Ref-iCC have positively charged surfaces, while FS-1HPC-NaOH-iCC is negatively charged. For the positively charged membranes, the retention sequences are consistent with Donnan exclusion: FS-Ref-STMP follows $MgCl_2$ > NaCl > $MgSO_4$ > Na_2SO_4 (Peeters et al., 1998; Kamp et al., 2021), and FS-Ref and FS-Ref-iCC show a similar sequence ($MgCl_2$ > NaCl ≈ $MgSO_4$ > Na_2SO_4). In a positively charged membrane, higher

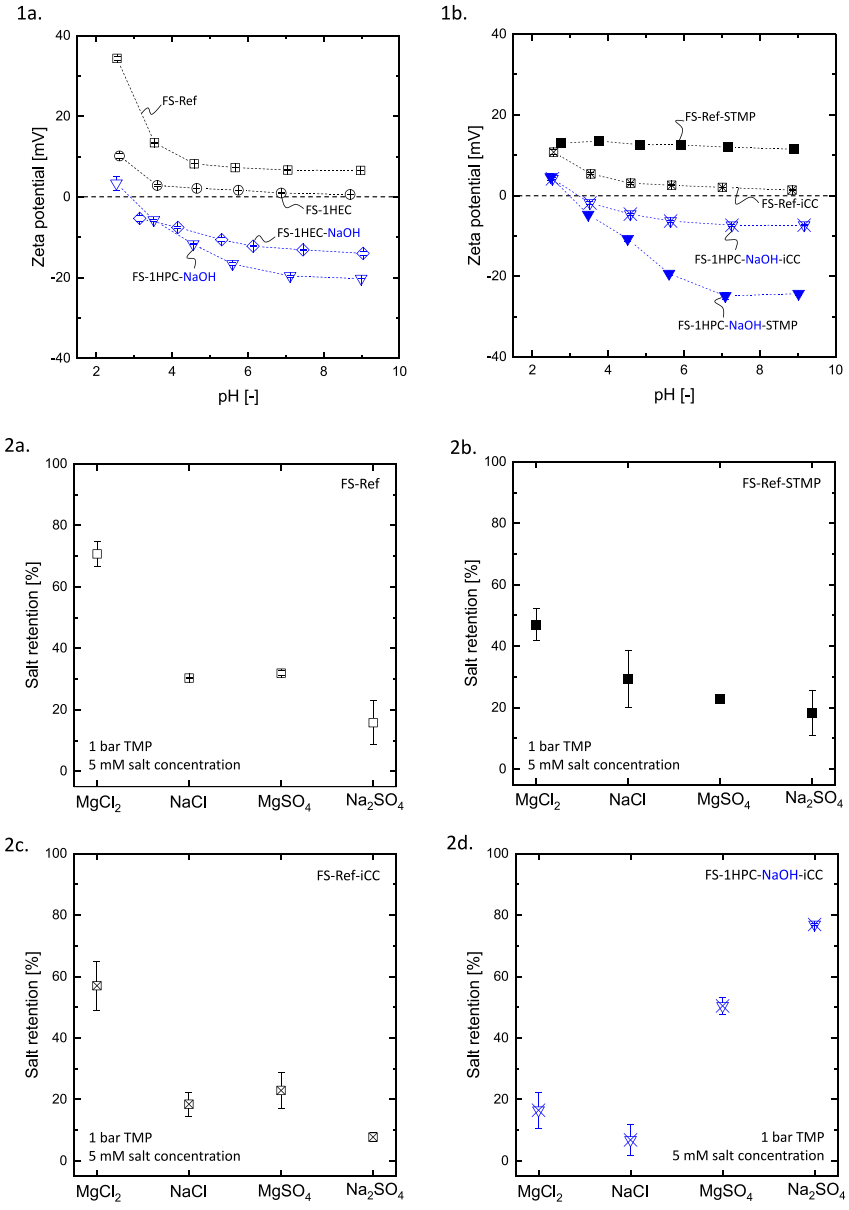

Fig. 4. Zeta potential of the membrane surface as a function of pH for the membrane FS-Ref, FS-1HEC, FS-1HEC-NaOH, and FS-1HPC-NaOH (1a.); zeta potential of the membrane surface as a function of pH for the membrane FS-Ref-STMP, FS-Ref-iCC, FS-1HPC-NaOH-STMP and FS-1HPC-NaOH-iCC (1b.); Salt retention of the membrane FS-Ref (2a.), FS-Ref-STMP (2b.), FS-Ref-iCC (2c.), and FS-1HPC-NaOH-iCC (2d.). The salt retention measurements were conducted in single separate salt retention measurements at TMP 1 bar and 5 mM salt concentration.

co-ion valence intensifies Donnan exclusion (e.g., Mg^{2+} *vs.* Na^{+}), leading to higher retention ($MgCl_2$ > NaCl), whereas higher counter-ion valence reduces retention (e.g., SO_4^{2-} *vs.* Cl^{-}), yielding NaCl > Na_2SO_4. The intermediate retention of $MgSO_4$ reflects the competing effects of a bivalent co-ion and a bivalent counter-ion (Schaep et al., 1999, 2001).

For the negatively charged FS-1HPC-NaOH-iCC membrane, the salt retention follows Na_2SO_4 > $MgSO_4$ > $MgCl_2$ > NaCl. This ordering aligns with Donnan expectations for co-ion valence: a higher anion valence increases retention (SO_4^{2-} > Cl^{-}) — and, in general, a higher counter-ion valence tends to decrease retention (Mg^{2+} < Na^{+}) (Schaep et al., 1999, 2001). However, the higher retention of $MgCl_2$ relative to NaCl indicates that dielectric and steric exclusion also contribute, consistent with the larger hydrated radius of Mg^{2+} compared with Na^{+} (Tansel et al., 2006).

4. Conclusion

This study demonstrates that HEC and HPC, used as cellulosic additives in the polymer solution, significantly tailor membrane properties. Key advances include enhanced and controllable porosity by varying the HEC content, improved mechanical stability of the fabricated PEC membranes, and finely tunable surface charge that can be shifted from positive or near-neutral to negative via NaOH pretreatment of the additives. In addition, STMP crosslinking further enhances the mechanical robustness of these PEC membranes.

We fabricated mechanically stable, free-standing PEC flat-sheet membranes spanning UF and MF: FS-1HEC and FS-1HEC-NaOH (1 wt% HEC; UF) and FS-2HEC (2 wt% HEC; MF). We also developed a PEC nanofiltration (NF) membrane (FS-1HPC-NaOH-iCC) using NaOH-pretreated HPC together with STMP coagulation crosslinking. This

membrane exhibits improved mechanical stability and a negatively charged surface, resulting in 77% retention of Na_2SO_4 and 7% retention of NaCl.

CRediT authorship contribution statement

Ang Zhao: Writing – review & editing, Writing – original draft, Visualization, Validation, Methodology, Investigation, Formal analysis, Data curation, Conceptualization. **Lea Erbacher:** Methodology, Investigation, Formal analysis. **Prasath Paskaran:** Methodology, Investigation, Formal analysis. **Matthias Wessling:** Writing – review & editing, Supervision, Resources, Project administration, Funding acquisition.

Declaration of Generative AI and AI-assisted technologies in the writing process

During the preparation of this work, ChatGPT and Grammarly were used to refine writing and improve readability. The authors meticulously reviewed and edited the AI-generated content as necessary, and take full responsibility for the content of this publication.

Declaration of competing interest

The authors declare the following financial interests/personal relationships which may be considered as potential competing interests: Matthias Wessling has patent pending to Rheinisch-Westf lische Technische Hochschule Aachen. If there are other authors, they declare that they have no known competing financial interests or personal relationships that could have appeared to influence the work reported in this paper.

Acknowledgments

The authors thank Karin Faensen for the high-quality FESEM images. Besides, the authors thank Daniela Wilhelm, Viktor Becker, and Maximilian Eickelmann Reyes for their support during their student thesis on this topic. M.W. acknowledges DFG funding through the Gottfried Wilhelm Leibniz Award 2019 (WE 4678/12-1). M.W. appreciates the support from the Alexander-von-Humboldt foundation, Germany.

Appendix A. Supplementary data

Supplementary material related to this article can be found online at https://doi.org/10.1016/j.memlet.2025.100110.

Data availability

Data will be made available on request.

References

Baig, M.I., Durmaz, E.N., Willott, J.D., de Vos, W.M., 2020. Sustainable membrane production through polyelectrolyte complexation induced aqueous phase separation. Adv. Funct. Mater. 30 (5), 1907344.
Bediako, J.K., Mouele, E.S.M., El Ouardi, Y., Repo, E., 2023. Saloplastics and the polyelectrolyte complex continuum: Advances, challenges and prospects. Chem. Eng. J. 462, 142322.
Boom, R., Wienk, I., Van den Boomgaard, T., Smolders, C., 1992. Microstructures in phase inversion membranes. Part 2. The role of a polymeric additive. J. Membr. Sci. 73 (2–3), 277–292.
Cabasso, I., Klein, E., Smith, J.K., 1976. Polysulfone hollow fibers. I. Spinning and properties. J. Appl. Polym. Sci. 20 (9), 2377–2394.
Durmaz, E.N., Baig, M.I., Willott, J.D., de Vos, W.M., 2020. Polyelectrolyte complex membranes via salinity change induced aqueous phase separation. ACS Appl. Polym. Mater. 2 (7), 2612–2621.
Emonds, S., Kamp, J., Borowec, J., Roth, H., Wessling, M., 2021. Polyelectrolyte complex tubular membranes via a salt dilution induced phase inversion process. Adv. Eng. Mater. 23 (5), 2001401.
Hwang, J.R., Sefton, M.V., 1995. The effects of polymer concentration and a pore-forming agent (PVP) on HEMA-MMA microcapsule structure and permeability. J. Membr. Sci. 108 (3), 257–268.
Kamp, J., Emonds, S., Borowec, J., Toro, M.A.R., Wessling, M., 2021. On the organic solvent free preparation of ultrafiltration and nanofiltration membranes using polyelectrolyte complexation in an all aqueous phase inversion process. J. Membr. Sci. 618, 118632.
Kim, J.H., Min, B.R., Park, H.C., Won, J., Kang, Y.S., 2001. Phase behavior and morphological studies of polyimide/PVP/solvent/water systems by phase inversion. J. Appl. Polym. Sci. 81 (14), 3481–3488.
Koyuncu, I., Sengur, R., Turken, T., Guclu, S., Pasaoglu, M., 2015. Advances in water treatment by microfiltration, ultrafiltration, and nanofiltration. In: Advances in Membrane Technologies for Water Treatment. Elsevier, pp. 83–128.
Li, J., Li, L., Brink, H., Allegri, G., Lindhoud, S., 2025. Polyelectrolyte complex-based materials for separations, progress, challenges and opportunities. Mater. Horizons.
Michaels, A.S., 1965. Polyelectrolyte complexes. Ind. Eng. Chem. 57 (10), 32–40.
Peeters, J., Boom, J., Mulder, M., Strathmann, H., 1998. Retention measurements of nanofiltration membranes with electrolyte solutions. J. Membr. Sci. 145 (2), 199–209.
Schaep, J., Vandecasteele, C., Mohammad, A.W., Bowen, W.R., 1999. Analysis of the salt retention of nanofiltration membranes using the donnan–steric partitioning pore model. Sep. Sci. Technol. 34 (15), 3009–3030.
Schaep, J., Vandecasteele, C., Mohammad, A.W., Bowen, W.R., 2001. Modelling the retention of ionic components for different nanofiltration membranes. Sep. Purif. Technol. 22, 169–179.
Shamoun, R.F., Reisch, A., Schlenoff, J.B., 2012. Extruded saloplastic polyelectrolyte complexes. Adv. Funct. Mater. 22 (9), 1923–1931.
Tansel, B., Sager, J., Rector, T., Garland, J., Strayer, R.F., Levine, L., Roberts, M., Hummerick, M., Bauer, J., 2006. Significance of hydrated radius and hydration shells on ionic permeability during nanofiltration in dead end and cross flow modes. Sep. Purif. Technol. 51 (1), 40–47.
Wang, Q., Schlenoff, J.B., 2014. The polyelectrolyte complex/coacervate continuum. Macromolecules 47 (9), 3108–3116.
Yakin, F.E., Barisik, M., Sen, T., 2020. Pore size and porosity dependent zeta potentials of mesoporous silica nanoparticles. J. Phys. Chem. C 124 (36), 19579–19587.
Yoo, S.H., Kim, J.H., Jho, J.Y., Won, J., Kang, Y.S., 2004. Influence of the addition of PVP on the morphology of asymmetric polyimide phase inversion membranes: effect of PVP molecular weight. J. Membr. Sci. 236 (1–2), 203–207.